The ERIS adaptive optics system

Enrico Marchetti*[a], Enrico Fedrigo[a], Miska Le Louarn[a], Pierre-Yves Madec[a], Christian Soenke[a], Roland Brast[a], Ralf Conzelmann[a], Bernard Delabre[a], Michel Duchateau[a], Christoph Frank[a], Barbara Klein[a], Paola Amico[a], Norbert Hubin[a], Simone Esposito[b], Jacopo Antichi[b], Luca Carbonaro[b], Alfio Puglisi[b], Fernando Quirós-Pacheco[b], Armando Riccardi[b], Marco Xompero[b]

[a]European Organization for Astronomical Research in the Southern Hemisphere, Karl-Schwarzschild-Str. 2, D-85748 Garching bei München, Germany
[b]INAF-Osservatorio Astrofisico di Arcetri, Largo Enrico Fermi 5, I-50125 Firenze, Italy

ABSTRACT

The Enhanced Resolution Imager and Spectrograph (ERIS) is the new Adaptive Optics based instrument for ESO's VLT aiming at replacing NACO and SINFONI to form a single compact facility with AO fed imaging and integral field unit spectroscopic scientific channels. ERIS completes the instrument suite at the VLT adaptive telescope. In particular it is equipped with a versatile AO system that delivers up to 95% Strehl correction in K band for science observations up to 5 micron

It comprises high order NGS and LGS correction enabling the observation from exoplanets to distant galaxies with a large sky coverage thanks to the coupling of the LGS WFS with the high sensitivity of its visible WFS and the capability to observe in dust embedded environment thanks to its IR low order WFS. ERIS will be installed at the Cassegrain focus of the VLT unit hosting the Adaptive Optics Facility (AOF). The wavefront correction is provided by the AOF deformable secondary mirror while the Laser Guide Star is provided by one of the four launch units of the 4 Laser Guide Star Facility for the AOF. The overall layout of the ERIS AO system is extremely compact and highly optimized: the SPIFFI spectrograph is fed directly by the Cassegrain focus and both the NIX's (IR imager) and SPIFFI's entrance windows work as visible/infrared dichroics.

In this paper we describe the concept of the ERIS AO system in detail, starting from the requirements and going through the estimated performance, the opto-mechanical design and the Real-Time Computer design.

Keywords: Adaptive Optics, Shack-Hartmann Wavefront Sensor, Pyramid Wavefront Sensor, Deformable Secondary Mirror, Laser Guide Stars, Astronomical Instrumentation, Infrared Wavefront Sensor

1. INTRODUCTION

ERIS[1] is the new IR instrument for the Adaptive Optics Facility[2] (AOF) to be installed at the Cassegrain focus of VLT's UT4. It consists of an AO module comprising the wave front sensors (WFS) and the Real-Time Computer (RTC), feeding SPIFFI, the Integral Field Unit spectrograph currently included in the SINFONI[3] instrument, and NIX the new near-infrared imaging camera that is supposed to take over some of the most used observing modes of NACO[4].

ERIS performs high spatial resolution spectroscopic and imaging observations at infrared (IR) wavelengths enabled by high Strehl AO correction on a narrow Field of View (FoV).

ERIS uses and depends on the AOF infrastructure to perform the narrow FoV AO correction and its implementation maximizes the re-use of existing sub-systems and components developed in the framework of the AOF. In particular, the AO correction is provided by the AOF Deformable Secondary Mirror (DSM) and the artificial Laser Guide Stars (LGSs) are generated by the Four Laser Guide Star Facility (4LGSF) system. Natural Guide Stars (NGS) are also used for specific observations.

In this paper we present the design of the ERIS AO system (hereafter refereed as ERIS AO module). Starting from the AO module requirements the AO module performance obtained via dedicated numerical simulations will be described. Then the opto-mechanical design and the real-time computer design.

*emarchet@eso.org; phone +49 89 32006458; fax +49 89 3202362

2. AO MODULE REQUIREMENTS

The design of ERIS AO module is done according to the ERIS Top-Level Requirements (TLRs). The TLRs most relevant for the AO design are the following:

- ERIS shall be mounted at UT4 Cassegrain.

- The AO module shall feed both the imaging camera and the spectrograph

- The AO module shall use the DSM and anyone of the four AOF lasers.

- The AO module shall perform:

  o On axis correction on an NGS

  o On axis correction on an LGS

  o LGS correction shall be assisted by visible and IR low order wavefront correction

- The AO module shall deliver under standard atmospheric conditions (0.87 arcsec seeing) over 15min duration the average Strehl ratio at 2.2 μm:

  o For NGS wavefront sensing:$\geq$75 % in the direction of the NGS (on-axis) for an m_R=8 star (class G2). For a m_R=13 and 15 the Strehl ratio shall be respectively 60% and 35%. Off-axis performance follows anisoplanatism.

  o For LGS wavefront sensing with visible NGS: $\geq$60% in the direction of the LGS (on-axis) for a m_R=12 on-axis low order correction NGS (class G2). For a m_R=17 and 19 the Strehl ratio shall be respectively 55% and 35%. On-axis performance with off-axis low order correction NGS follows atmospheric tip-tilt anisoplanatism.

  o For LGS wavefront sensing with near-IR NGS: $\geq$60% (TBC) in the direction of the LGS (on-axis) for a mK=10 star (class G2). On-axis performance with off-axis low-order correction NGS follows atmospheric tip-tilt anisoplanatism.

- For LGS wavefront sensing the unrestricted search field (including the instrument field centre) for the visible low-order correction NGS shall allow to find a $m_R$$\leq$17 star (class G2) in at least 30% of the pointings at the Galactic pole.

The derived guidelines for the AO module design can be summarized as following:

- The AO module is designed to be accommodated at the UT4 **Cassegrain** and to minimize the impact of instrumental perturbations (for example flexures) on the correction performance.

- The AO module makes use of the AOF's **DSM** (1170 actuators) for correcting the on-axis atmospheric turbulence.

- The AO module makes use of at least **one laser and launch telescope of the 4LGSF** to generate the LGS wavefront sensing source.

- The AO module is equipped with **one high order NGS wavefront sensor** for on-axis atmospheric turbulence correction. The number of sub-apertures should be dimensioned in order to fully exploit the DSM correction capabilities guaranteeing high Strehl ratio performance.

- The AO module is equipped with **one high order LGS wavefront sensor** for on-axis atmospheric turbulence correction. The number of sub-apertures and the FoV should be dimensioned in order to fully exploit the DSM correction capabilities and to cope with the LGS post elongation to guarantee high Strehl ratio performance.

- The AO module is equipped with **one low order visible NGS wavefront sensor** supporting the LGS wavefront sensor to compensate for tip-tilt indetermination due to the LGS use. The number of sub-apertures should be dimensioned to guarantee both the most precise low order correction and the accessibility to the faintest wavefront sensing sources. The NGS searching FoV is dimensioned to achieve the required sky coverage.

- The AO module is equipped with **one low order near-IR NGS wavefront sensor** supporting the LGS wavefront sensor to compensate for tip-tilt indetermination due to the LGS use. The number of sub-apertures should be dimensioned to guarantee both the most precise low order correction and the accessibility to the faintest wavefront sensing sources.

After a careful trade off phase the following system main characteristics have been set:

- High Order **NGS WFS: the Pyramid WFS (PWFS)**, 40×40 sub-apertures.

- High Order **LGS WFS: the Shack-Hartmann WFS (SHWFS)**, 40×40 sub-apertures (identical copy of the WFSs used for the AOF).

- Low Order **visible NGS WFS: the Pyramid WFS** 2×2 sub-apertures (it is the high order NGS WFS used in a different configuration).

- Low Order **near-IR NGS WFS: Shack-Hartmann WFS** 2×2 sub-apertures.

In order to maximize re-using of existing sub-systems and components developed in the framework of the AOF, the following key components have been identified for the design of the AO module:

- **WFS CCD cameras: CCD220** used as standard detector for the AOF LGS WFSs and visible NGS low order sensors;

- **WFS CCD camera controllers**: ESO's standard **New General detector Controller (NGC)** used by AOF and by all future ESO instruments;

- **Real-Time Computer: SPARTA**[5] platform used by AOF. SPARTA functionalities and features can be massively re-used for the AO module implementation.

3. ADAPTIVE OPTICS PERFORMANCE

In order to evaluate the ERIS AO module correction performance and sensitivity to main input parameters a complete set of numerical simulations have been performed with the ESO AO simulations tools OCTOPUS[6]. The simulations constitute the end-to-end modeling of all the steps involving the AO system main functionality and the input disturbance generation and propagation. The input parameters are the following:

Deformable Secondary Mirror configuration
- AOF DSM real geometry, 1170 actuators

High Order NGS WFS configuration
- Pyramid WFS, 40×40/20×20/10×10 sub-ap, 2.5 arcsec FoV diameter
- Central sensing wavelength: 0.7 μm

High Order LGS WFS configuration
- Shack-Hartmann, 40×40 sub-ap, 6×6 px/sub-ap, 0.83 arcsec/px
- Central sensing wavelength: 0.589 μm

Low Order visible NGS WFS configuration
- Pyramid, 2×2 sub-ap, 2.5 arcsec FoV diameter
- Central sensing wavelength: 0.7 μm

Low Order near-IR NGS WFS configuration
- Shack-Hartmann, 2×2 sub-ap, 8×8 px/sub-ap, 0.060 arcsec/px
- Central sensing wavelength: 2.2 μm

WFS detector characteristics
- Visible detector RON: 1.0 e⁻/px/frame (or e⁻/binned pixel/frame)
- Visible detector Dark: 1.2 e⁻/px/s (including the Clock-Induced Charge)

- Visible detector excess noise: $\sqrt{2}$
- Visible detector charge diffusion: FWHM 0.55 px
- IR detector RON: 4.0 e$^-$/px/frame
- IR detector Dark: 300 e$^-$/px/s

LGS related characteristics
- LGS launch location: Δx=1250 mm, Δy=5350 mm (with respect to the pupil/M1 center)
- LGS flux: 8×10^4 detected photons/s/sub-ap (without considering the excess noise)
- LGS spot size: 1.3 arcsec FWHM (small axis), short exposure
- LGS spot residual jitter: 120 mas rms, random Gaussian (quadratic sum of two orthogonal axes)
- Sodium profile: Gaussian, 10 km FWHM

Control loop characteristics
- High order WFS (NGS and LGS) reconstruction modal basis: Karhunen-Loeve
- High (NGS and LGS) and Low order WFS (NGS) loop maximum frequency: 1.0 kHz
- High (NGS and LGS) and Low order WFS (NGS) control loop delay: 1 to 3 depending on loop frequency
- Loop controller: simple integrator
- Shack-Hartmann centroiding algorithm: weighted centroid of gravity

Telescope pupil
- Diameter: 8m
- Central obstruction: 0.14 (linear ratio)

Sky background
- Visible sky background: 3300 detected photons/s/VLT-pupil/arcsec^2
- IR sky background: 8×10^5 photons/s/VLT-pupil/arcsec^2

Atmospheric conditions
The atmospheric conditions used for the simulations are: seeing 0.87 arcsec (at 500nm, 30 degrees off Zenith), labeled as "DIMM seeing 0.8 arcsec".

- Fried parameter (r_0): 0.119 m
- Outer Scale (L_0): 22 m
- Coherence time (τ_0): 3.0 ms

The atmosphere is made of 10 layers (see Table 1):

Table 1. Atmospheric model sued for the ERIS AO module simulations

Layer number	1	2	3	4	5	6	7	8	9	10
Height (m)	1.16* 30	1.16* 140	1.16* 281	1.16* 562	1.16* 1125	1.16* 2250	1.16* 4500	1.16* 7750	1.16* 11000	1.16* 14000
C_n^2 fraction	0.59	0.02	0.04	0.06	0.01	0.05	0.09	0.04	0.05	0.05
Speed (m/s)	6.6	5.9	5.1	4.5	5.1	8.3	16.3	30.2	34.3	17.5

Other seeing values have been used in the simulations for the extended performance evaluation. They are labeled "DIMM seeing 0.6-1.0-1.2 arcsec".

The high order NGS PWFS on-axis performance vs. NGS magnitude is shown in Figure 1. The sampling is 40×40 at bright flux down to 10×10 for the faintest flux. The maximum loop frequency is 1.0 kHz (bright flux) down to 300 Hz (faintest flux).
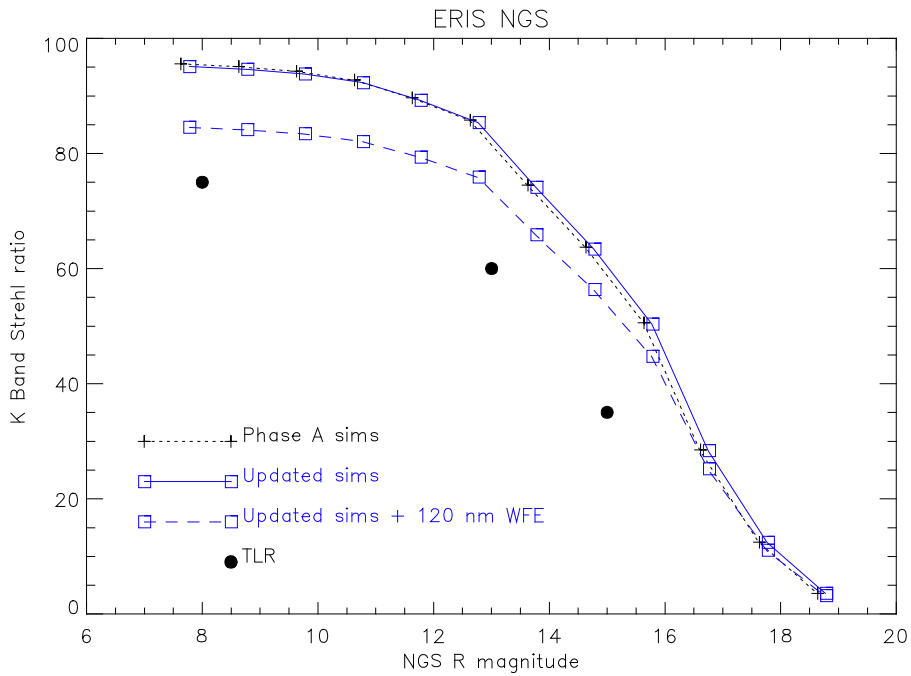
Figure 1. On-axis NGS WFS correction performance updated for the design changes occurred after the ERIS Phase A. Related TLR values are also shown.

The high order LGS SHWFS on-axis performance vs. on-axis low order visible NGS magnitude is shown in Figure 2. The loop frequency goes from 1.0 kHz for the brightest flux down to 100 Hz for the faintest point of the curves.
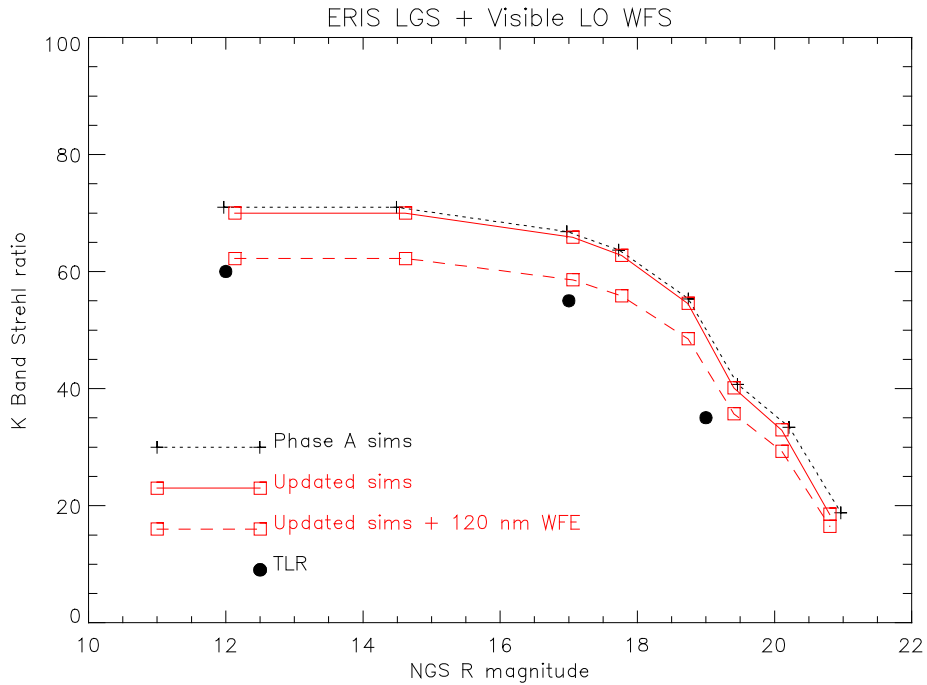

Figure 2. On-axis LGS WFS with visible low order WFS (NGS on-axis) correction performance updated for the design changes occurred after the ERIS Phase A. Related TLR values are also shown.

The high order LGS SHWFS on-axis performance vs. on-axis low order IR NGS magnitude is shown in Figure 3. The loop frequency goes from 1.0 kHz for the brightest flux down to 100 Hz for the faintest point of the curves.
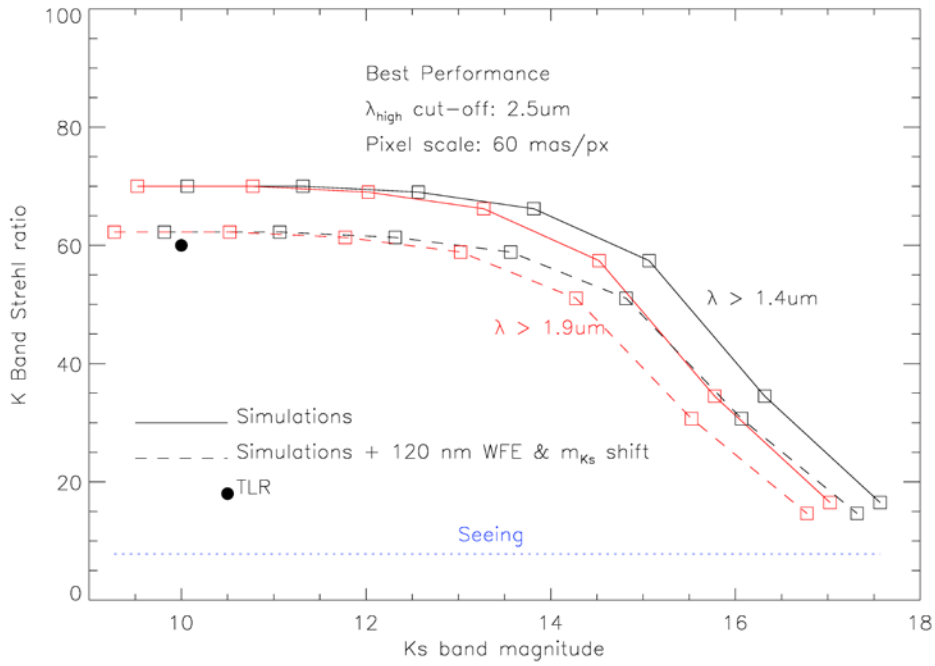

Figure 3. On-axis LGS WFS with IR low order WFS (NGS on-axis) correction performance with and without WFE budget. The related TLR value is also shown.

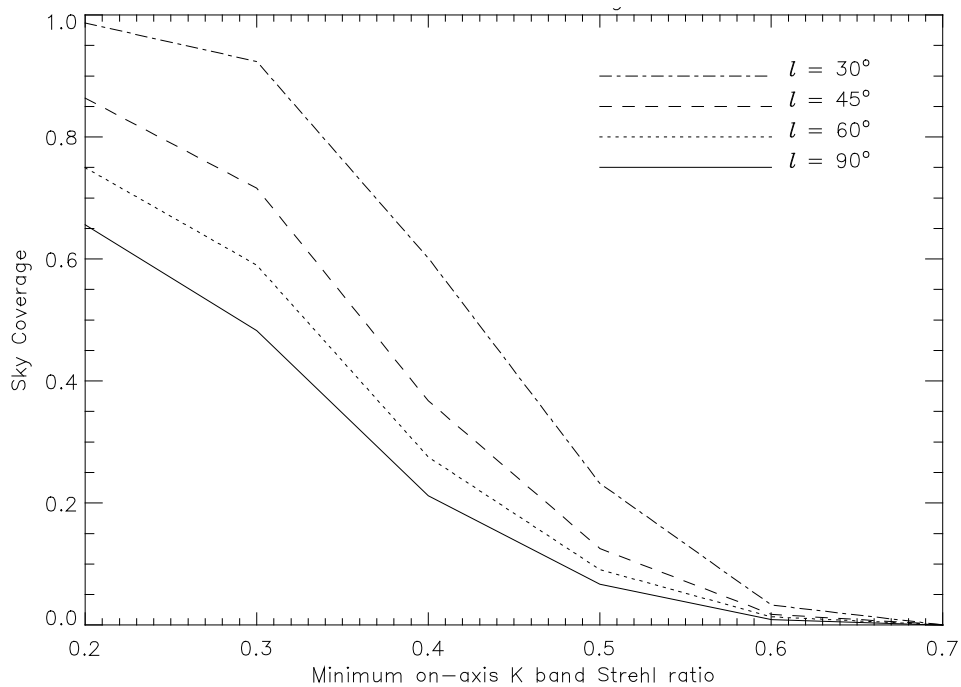The sky coverage for the LGS mode at different Galactic latitudes is shown in Figure 4.

Figure 4. LGS mode sky coverage vs. on-axis Strehl for different galactic latitudes. Performance are for "DIMM seeing 0.8 arcsec".

4. ADAPTIVE OPTICS DESIGN

The ERIS AO module is located inside the ERIS supporting structure which is hosting the IR camera and providing an interface for the spectrograph SPIFFI (see Figure 5, left). The AO bench is supporting the common optics, the NGS, the LGS, the low order IR WFSs and the calibration unit. A view of the AO bench is given in Figure 5, right. The light coming from the telescope is back reflected by either the MIX's or the SPIFFI entrance windows which are also Vis/IR dichroics (transmitted λ>1.0 μm, reflect λ<1.0 μm). SPIFFI is fed straight through while NIX requires the insertion of a folding mirror.
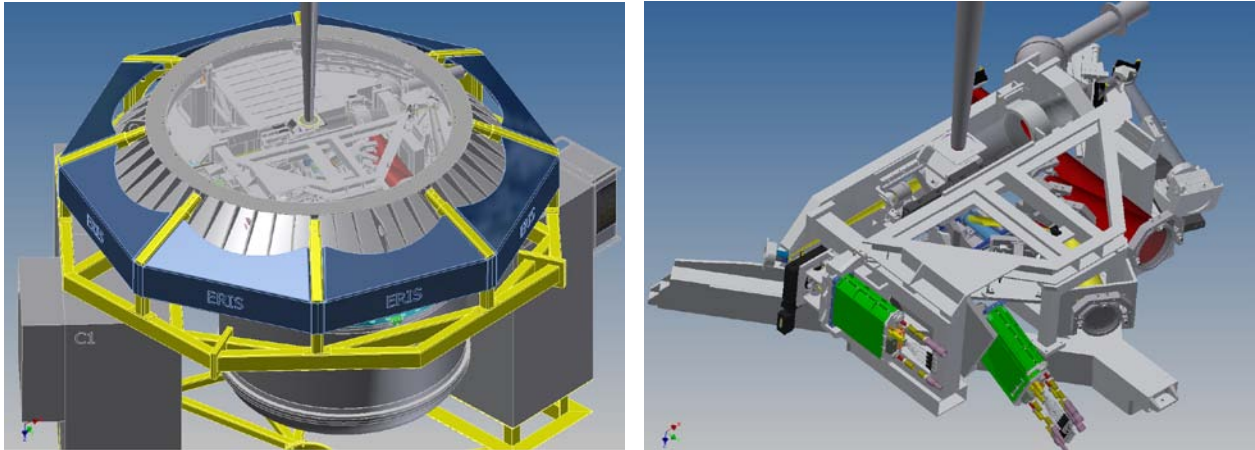

Figure 5. Left: ERIS assembly. The AO module is located on a bench inside the ERIS supporting structure. Right: ERIS AO module.

4.1 NGS WFS path

The NGS WFS is built by the Osservatorio Astrofisico di Arcetri[7]. The 3D view of the NGS WFS path is show in Figure 6. The 2 arcmin diameter FoV visible light beam reflected by one of the entrance windows of the two instruments enters the AO module and it is separated by another dichroic transmitting the Sodium wavelength (λ =0.589 μm, $\Delta\lambda$ ~15 nm) toward the LGS WFS and reflecting the rest toward the NGS WFS.
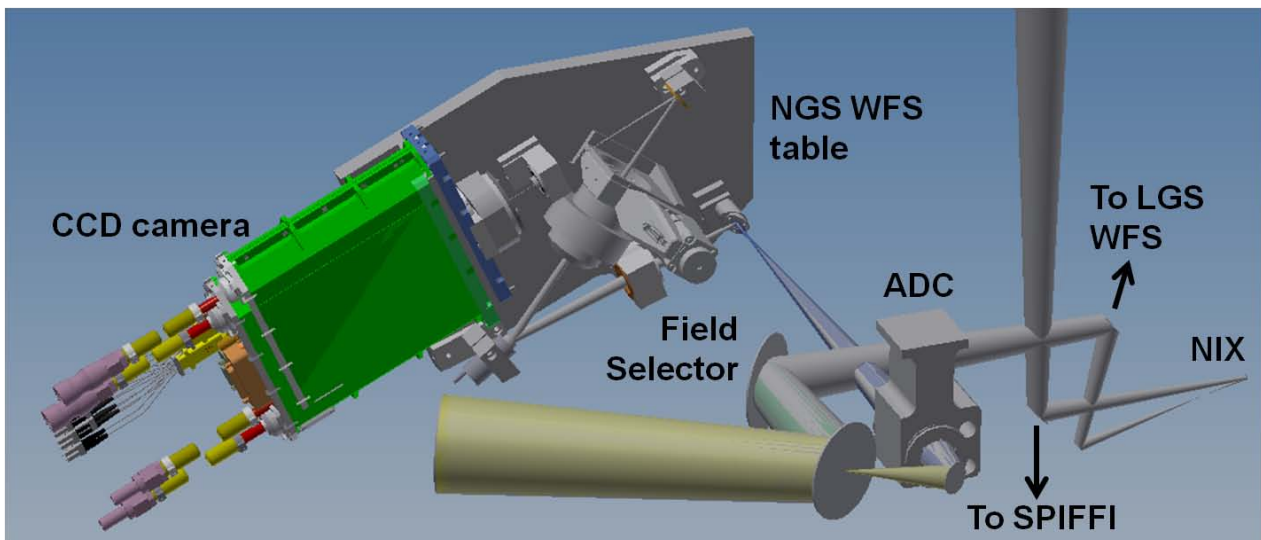

Figure 6. NGS WFS path.

The beam forms a pupil image (thanks to the concave entrance windows of the instruments) on a field selector mirror that is able to bring any reference source in 2 arcmin diameter FoV at the center of the NGS WFS FoV (31% sky coverage at the Galactic pole). The field selector provides to re-acquire the NGS during observations when jittering (small and large offsets) is implemented. The field selector is also driven during observations to compensate for the image drift between visible (AO WFS) and IR (science instruments) wavelengths due to the differential atmospheric dispersion and for the instrument flexures. From the Field Selector on the transmitted FoV is 5 arcsec diameter.
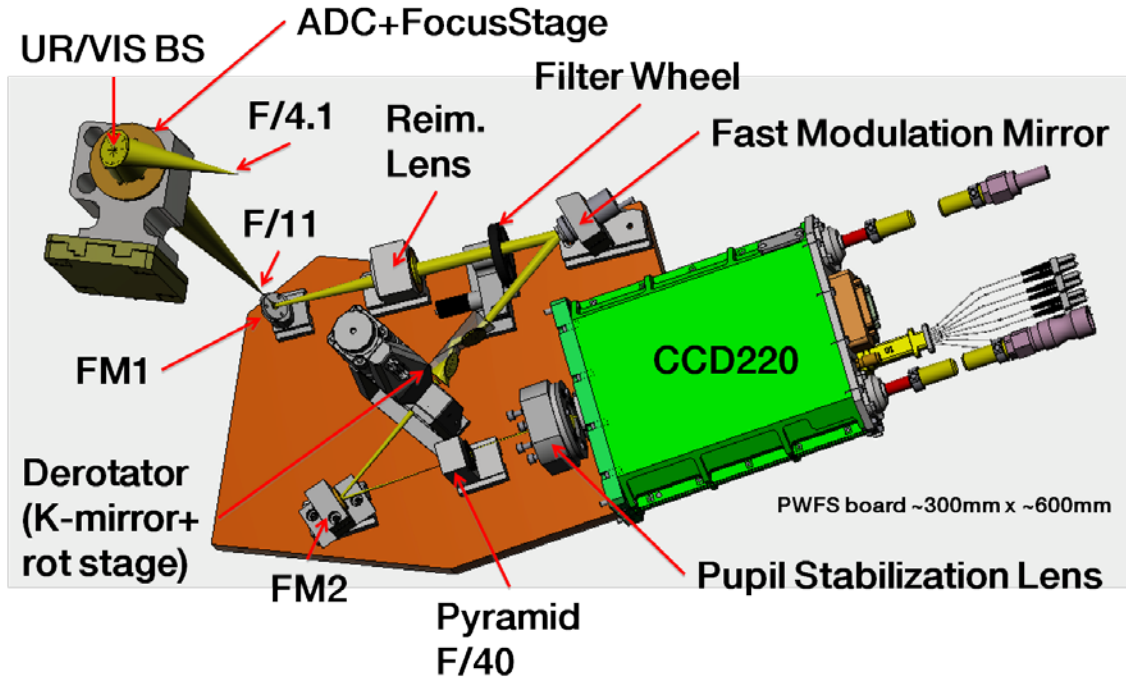

Figure 7. NGS WFS table.

An optical system of two mirrors reimages a second pupil where the ADC is located. Just before the ADC a second visible/IR dichroic reflects the light toward the NGS WFS: its purpose is to feed the low order IR WFS which follows a different path. The ADC includes also a re-imaging lens to create and intermediate focal plane and a focusing stage.

The beam then enters the NGS WFS table (see Figure 7) which includes a Fast Jitter Mirror for modulating the NGS on the pyramid tip, and optical derotator to compensate for the rotation of the DSM's image on the NGS WFS plane (the ERIS instrument rotates with the scientific FoV), the optical pyramid, the pupil stabilization lens and the CCD220 camera. Two additional lenses and two folding mirrors assure the compactness of the whole assembly. Finally a filter wheel is included in the optical path to enable the dimming of the light from the brightest stars and to narrow the FoV.

4.2 High order WFS description

The High Order NGS WFS is the Pyramid WFS. The incoming light is split in four slightly diverging sub-beams by a refractive pyramid. A lens assembly re-images for each beam the telescope pupil (0.960 mm diameter) on the detector. The maximum transmitted FoV is 3.5 arcsec diameter.

The pixels of the detector act as sub-apertures: each pupil is mapped by 40×40 pixels equivalent to 40×40 sub-apertures. The number of sub-apertures can be reduced down to 10×10 by binning the detector pixels before reading them out (4×4 binning).

For closed loop operations the image of the NGS reference source is modulated along a circular path around the tip of the refractive pyramid by means of the fast jitter mirror. The amplitude of the modulation is selected by the user according to seeing condition and NGS reference source magnitude. The speed of the modulation is locked to the detector integration time and synchronized by the detector controller: always one full modulation loop per integration time. The maximum detector frame rate is 1000 Hz.

The stabilization of the pupil image on the detector is guaranteed by the ancillary loop driving the Pupil stabilization mirror. The main characteristics of the High Oder PWFS are listed in Table 3.

Table 3. High order NGS WFS main parameters

Parameter	Value	Note
n. of pupils	4	-
FoV	3.5 arcsec diameter	-
n. of sub-apertures per pupil	40×40... 10×10	Binning 1×1...4×4
Pixels per sub-aperture per pupil	1×1	Binned pixel
Pupil size	0.960 mm	-
Detector	CCD220	-
Maximum frame rate	1000 Hz	-
Modulation type – amplitude	Circular – 0...10×λ/D	User defined
Modulation speed	= detector integration time	-

4.3 Low order NGS WFS description

All the functionalities of the Low Order NGS WFS are provided by the High Order PWFS, in fact the High Order PWFS works also as Low Order NGS. The only difference consists in the number of sub-apertures. In order to measure the tip-tilt and the focus the Low Order NGS WFS has 2×2 sub-apertures per pupil. The smaller number of sub-apertures is obtained by binning the pixels before reading them out (20×20 binning). The main characteristics of the low order NGS WFS are listed in Table 4.

Table 4. Low order NGS WFS main parameters

Parameter	Value	Note
n. of pupils	4	-
FoV	3.5 arcsec diameter	-
n. of sub-apertures per pupil	2×2	Binning 20×20
Pixels per sub-aperture per pupil	1×1	Binned pixel
Pupil size	0.960 mm	-
Detector	CCD220	-
Maximum frame rate	1000 Hz	-
Modulation type – amplitude	Circular – 0...10×λ/D	User defined
Modulation speed	= detector integration time	-

4.4 LGS WFS path

The 3D view of the LGS WFS path is shown in Figure 8. The Sodium light (λ=0.589 µm, $\Delta\lambda$ ~15 nm TBC) transmitted by the dichroic is folded toward the LGS zoom. The LGS zoom compensates the variation of the LGS distance due to the telescope elevation angle (from 80 to 240 km). The focus compensator is also used to finely adjust the variations of the LGS mean altitude variations due to the change of the Sodium vertical profile structure. As for the NGS WFS, an optical derotator compensates for the rotation of the DSM's image on the LGS WFS focal plane. The transmitted FoV is 5 arcsec diameter.

A pupil stabilization mirror is located at the intermediate focal plane created by the zoom. The scope of this function is to compensate for the DSM image shift on the LGS WFS. After the pupil stabilization mirror a collimator reimages a telescope pupil of 5.760 mm on a lenslet array with a focal length of 4.217 mm. The lenslet array is glued on the WFS camera window. The Shack-Hartmann spots are imaged directly on the CCD220 detector plane.
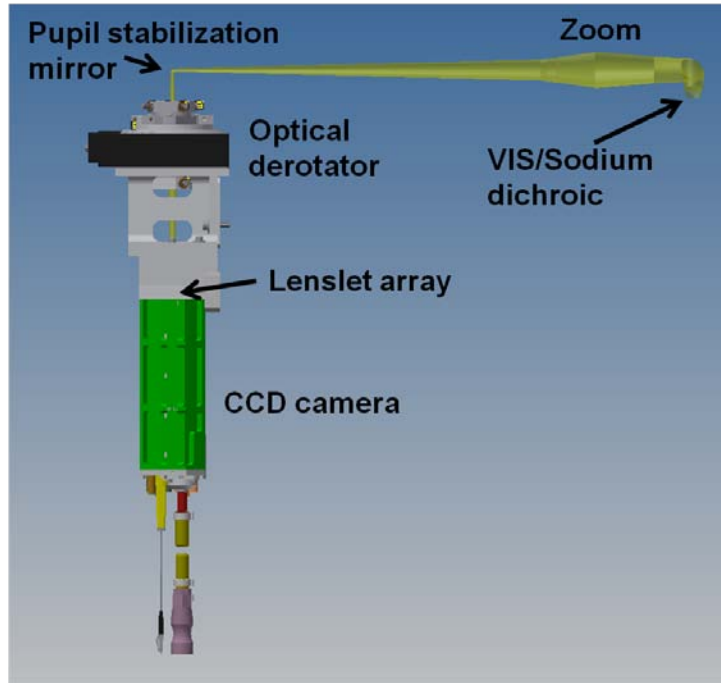
Figure 8. LGS WFS optical path.

4.5 High order LGS WFS description

The High Order LGS WFS is a Shack-Hartmann WFS identical copy of the AOF LGS WFSs. The transmitted FoV is 5 arcsec diameter. The number of sub-apertures is 40×40, 6×6 pixels each, so the full CCD220 detector area is used.The maximum detector frame rate is 1000 Hz.

The stabilization of the pupil image on the lenslet array is guaranteed by the ancillary loop driving the Pupil stabilization mirror. The main characteristics of the High Oder LGS WFS are listed in Table 5.

Table 5. High order LGS WFS main parameters

Parameter	Value
FoV	5 arcsec diameter
n. of sub-apertures	40×40
Pixels per sub-aperture per pupil	6×6
Pixel scale	0.83 arcsec/pixel
Pupil size	5.760 mm
Lenslet pitch	0.144 mm
Lenlset focal length	4.217 mm
Detector	CCD220
Maximum frame rate	1000 Hz

4.6 IR low order WFS path

The optical layout of the IR low order WFS has been already shown in Figure 9. The IR NGS low order WFS light path generates out of the entrance beam, before the reaching the instruments, via a dichroic reflecting 20% (TBC) of the light > 1.0 µm and transmitting all the rest (i.e. 100% of visible light and 80% of IR light) and it can be inserted when this specific ERIS AO mode is required. The IR low order WFS path uses the same field selector of the visible NGS WFS path for acquiring the targets within 2 arcmin FoV. Part of the path is common with the one of the visible NGS WFS a second dichoric (transmitting the IR and reflecting the Visible) provides the final wavelength separation before reaching

the IR WFS camera. The optical concept for the IR WFS camera includes a cold field stop, a pupil lens and a 2×2 lenslet array at the pupil position, with proper masking to act as pupil cold stop.

4.7 Low order IR WFS description

The wavefront sensor type has been chosen to be a 2×2 Shack-Hartmamn WFS. This choice has been done in the framework of both mitigating the risk associated to its development and to minimize the effort required for its implementation. In fact such a WFS configuration is identical to the one of IRLOS, the IR low order sensor of the AOF GALACSI Narrow Field Mode. The main characteristics of the Low Oder IR WFS are listed in Table 6.

Table 6. High order LGS WFS main parameters

| IR low order WFS Parameter	Value	Note
Type	Shack-Hartmann	-
n. of sub-apertures	2×2	-
Minimum window for centroiding	8×8	Up to 160×128 for acquisition
Pixel scale	0.060 "/pixel	-
FoV of minimum window	0.480"	Up to 9.60" ×7.68" for acquisition
Detector type	Saphira	Sensitivity from 1.4 to 2.5 μm
Detector pixels size	24 μm	
Wavelength range	1.4-2.5 μm	-
Maximum frame rate	1000 Hz	-
Operating temperature	80°K	TBC
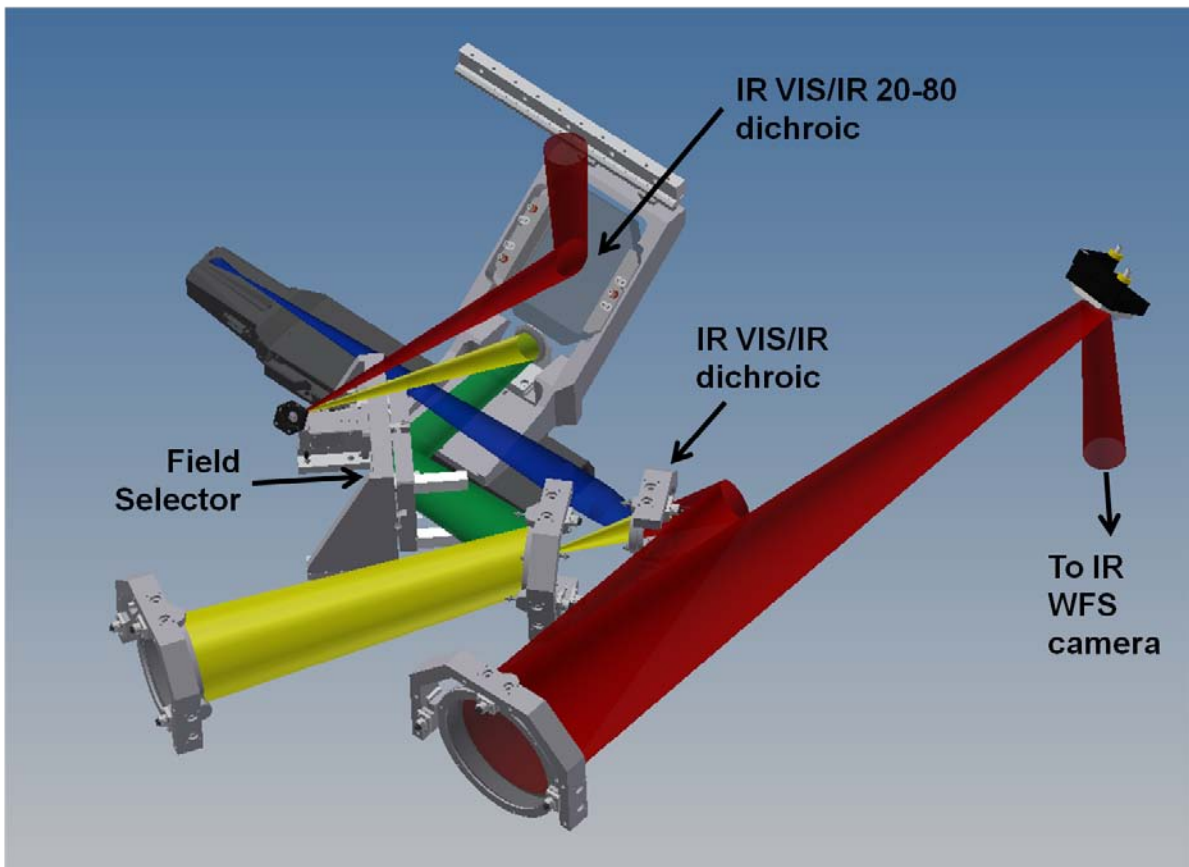
Figure 9. LGS WFS optical path.

4.8 WFS cameras

Visible WFS camera

The WFS sensor cameras for the LGS and NGS WFSs consist of the CCD220 package attached to the ESO front end electronics, in its mechanical housing. The CCD220 package is made of the mechanical package itself, housing the focal plane array and sealed by a Sapphire window. The CCD220 is an Electron Multiplying CCD detector (EMCCD) where the accumulated charge created by the incident photons is amplified by the impact ionization during the transfer across several stages of a dedicated register. When the amplified charge is read-out the associated noise (RON), which is not amplified, becomes negligible with respect the signal. EMCCD allows equivalent RON much smaller than 1e-/px/frame. The main characteristics of the CCD220 are listed in Table 7.

Table 7. CCD220 main characteristics

Parameter	Value	Note
Image area	5.76×5.76 mm	-
Image section active pixels	240 (H) $\times$ 240 (V)	-
Image pixel size	24×24 μm	-
Additional transition rows	2	-
Number of output amplifiers	8	-
Fill factor	100%	-
Peak charge storage (image area)	300 ke$^-$/px	@ gain =1
Dark signal	1.0 e$^-$/px/s	Average on meas. on 18 chips
RON (gain 1)	90 e$^-$/px/frame	Average on meas. on 18 chips
Max multiplication register gain	1000	-
Excess noise factor	$\sqrt{2}$	-

IR WFS camera

The baseline detector selected is a Saphira developed by SELEX Galileo with Metal Organic Vapor Phase Epitaxy (MOVPE) technology. The Saphira detector is designed for high speed infrared applications and is the result of a three year research and development programme alongside the European Southern Observatory on sensors for astronomical instruments. The key drivers were to achieve market-leading photon sensitivity (<10 photons rms) and high speed, non-destructive readout (>10K frame/s). Saphira is an HgCdTe avalanche photodiode (APD) array incorporating a full custom ROIC. Most applications will be in the 1 to 2.5μm range or the 3 to 4.2 μm range. A key aspect of the array is the ability to perform multiple non-destructive readouts which can allow Fowler sampling or "down the slope" sampling to significantly reduce the noise and increase the sensitivity. The architecture allows multiple, independently resettable windows and a selectable number of parallel outputs up to 32. The main characteristics of the Saphira detector WFS are listed in Table 8.

Table 8. Saphira detector main characteristics

Parameter	Value	Note
Image area	7.68×6.14 mm	-
Image section active pixels	320 (H) $\times$ 256 (V)	-
Image pixel size	24×24 μm	-
Number of parallel outputs	32	-
Peak charge storage (image area)	200 ke$^-$/px	@ gain =1
Conversion Gain	up to 40	-
RON (gain 1)	<4 e$^-$/px/frame	-
Excess noise factor	1	No excess noise
Full frame read-out	500 μs	32 px row is 200 ns
Read-out modes	Rolling-Reset and Read-Reset-Read	

5. REAL-TIME COMPUTER DESIGN

The ERIS Real-Time Computer (RTC) is based on ESOs Standard Platform for Adaptive Optics Real-Time Applications (SPARTA). At the time of writing SPARTA systems are already being used by three VLT 2nd generation instruments. The RTC for SPHERE is finalized and has been tested with SAXO in the lab including closure of all AO loops. The RTCs for the other two AOF AO systems GRAAL and GALACSI are currently under development.

5.1 Overview

The SPARTA RTC consists of two main building blocks:

- The RTC box: a 19" VXS chassis hosting a number of dedicated computing boards. The hard real-time AO loops are handled by this unit. All sensors and actuators are connected here

- The Co-processing cluster: a number of Linux servers which receive real-time data from the RTC box and handle all soft real-time functionalities like calibration, optimization, data recording, measurements and performance estimation

Both building blocks are interconnected through a dedicated private network.

The sensors and actuators connected to SPARTA are:

- LGS SHWFS: 240x240 pixels, 40x40 sub-apertures, 6x6 pixels per sub-aperture, max. frame rate 1000Hz, 1240 valid sub-apertures. This is the same sensor as already used with SPHERE. It has already been tested with SPARTA.

- NGS PWFS: configuration depending on mode. Most demanding configuration is: 240x240 pixels, 40x40 sub-apertures. Max. frame rate 1000Hz, 1256 valid sub-apertures. The IF between NGC and SPARTA is the same as for the LGS WFS.

- NGS IR low order WFS: configuration depending on mode. Most demanding configuration is: 320x256 pixels, 2x2 sub-apertures. Max. frame rate 1000Hz, 4 valid sub-apertures. The IF between NGC and SPARTA is the same as for the LGS WFS.

- DSM: 1170 actuators

- 4LGSF jitter actuators: 4 fast and 4 slow tip/tilt actuators (only one used in ERIS)

Note that the fast tip/tilt actuator for modulation in front of the PWFS and the pupil centering mirrors are not controlled by SPARTA.

The SPARTA system for ERIS will heavily re-use what has been developed for the existing systems.

5.2 Hardware design

The ERIS RTC box uses 3 processing boards:

- VPF1 acquisition: this board hosts the two WPUs for the SH WFS and the PWFS. In NGS mode, only the PWFS is used.

- T2V6 reconstruction: this board handles the projection of slopes into mirror space for the HO sensor (depending on mode LGS/NGS). In case on-the-fly matrix swapping with frame losses below 10 frames should be required, a second T2V6 board has to be added.

- VPF1 control: the operations on this board depend on the mode:

- NGS: delta positions are received from the T2V6 board and the IIR filter is applied. Mirror commands are sent to the DSM

- LGS: same as NGS but in addition, also the slopes from the LO NGS sensor are received, projected into DSM space, passed through an IIR filter and added to the control vector.

Data routing inside the RTC box and external fiber interfaces are handled by the CSW1 board.

The co-processing cluster will be made of the following components:

- 1 Dell PowerEdge R710 server: this is the machine known as the concentrator. It receives all real-time data from the RTC box, re-distributes it to the other cluster servers and is capable of recording real-time data on its internal RAID storage array.

- 2 Dell PowerEdge R610 servers: these machines handle processing tasks like calibration, optimization, statistics, etc…

- The RTC-box and the co-processing cluster will be interconnected via dedicated private networks. Therefore every host is connected to a CISCO 3750X switch.

- In addition, there will be a terminal server for access to the serial ports of all RTC box boards and a monitoring system for temperatures, voltages and fan status of the RTC box.

5.3 Software design

The SW architecture of the ERIS RTC is the same as for all other SPARTA systems. The difference is in the number and type of objects running in the co-processing cluster and their configuration.

Those objects providing general services like data distribution, recording, configuration management, disturbance injection and others exist – they are provided with the SPARTA common software. A number of objects already implemented for SPHERE, GRAAL or GALACSI can be reused – possibly with small adaptations. Examples would be the atmospheric statistics, performance estimation or the WFS optimization (dark following, flat measurement, etc…).

Certain objects which handle functionality specific to ERIS will have to be developed. These will mainly be related to the PWFS.

5.4 Performance estimation

The systems dimensions of the ERIS RTC are partly comparable to the ones of SPHERE (1240 sub-apertures, 1377 actuators, 1000Hz frame rate). Therefore, the following performance can be expected based on previous experience:

- LGS mode: 70µs from last pixel received to first command sent out (pure RTC delay)

- NGS mode: approx. 140 µs (due to the PWFS readout) from last pixel received to first command sent out (pure RTC delay)

6. CONCLUSIONS

The preliminary design of the ERIS AO module has been presented. The AO design has been derived from the instrument TLRs.

Detailed numerical simulations have been carried out to evaluate the system performance for its observing modes (NGS and LGS). The PWFS has been chosen as baseline for NGS WFS (high and low order) the advantage vs. classical SHWFS is on the significantly higher correction performance and the combination of high and low order allowing to reduce the number of WFSs on board.

The optical design has been presented for NGS, LGS and IR low order NGS paths. It has been proven that such AO architecture can fit in the reduced volume available at VLT Cassegrain focus. ERIS will benefit from AOF developments, namely DSM, 4LGSF and ancillary sub-systems such as SPARTA RTC, CCD220 WFS cameras and ESO controllers. In the specific the SPARTA design can, as of today, comfortably control the ERIS AO module with minor modifications related to PWFS implementation.

ERIS will deliver the highest ever achieved by any AO system in NGS mode, and will be extremely competitive in LGS mode especially for the sky coverage.

REFERENCES

[1] Kuntschner, H., et al., "ERIS: preliminary design phase overview," Proc. SPIE 9147, 9147-66 (2014).

[2] Arsenault, R., et al., "Manufacturing of the ESO adaptive optics Facility," Proc. SPIE 7736, 77360L-77360L-11 (2010).

[3] Bonnet, H., et al., "First Light of SINFONI at the VLT," Messenger 117, 17-24 (2004).

[4] Brandner, W., Rousset, G., Lenzen, R., Hubin, N., Lacombe, F., Hofmann, R., Moorwood, A., Lagrange, A.-M., Gendron, E., Hartung, M., Puget, P., Ageorges, N., Biereichel, P., Bouy, H., Charton, J., Dumont, G., Fusco, T., Jung, Y., Lehnert, M., Lizon, J.-L., Monnet, G., Mouillet, D., Moutou, C., Rabaud, D., Röhrle, C., Skole, S., Spyromilio, J., Storz, C., Tacconi-Garman, L., Zins, G., "NAOS+CONICA at YEPUN: First VLT Adaptive Optics System Sees First Light," Messenger 107, 1-6 (2002).

[5] Fedrigo, E., Donaldson, R., Suarez Valles, M., Soenke, C., Zampieri, S., Bourtembourg, R., "SPARTA for the VLT: status and plans," Proc. SPIE 7736, 77362I-77362I-10 (2010).

[6] Le Louarn, M., Verinaud, C., Korkiakoski, V., Fedrigo, E., "Parallel simulation tools for AO on ELTs," Proc. SPIE 5490, 705-712 (2004).

[7] Riccardi, A., Esposito, S., Antichi, J., Quirós-Pacheco, F., Puglisi, A., Carbonaro, L., Biliotti, V., Agapito, G., Briguglio, R., Di Rico, G., Dolci, M., Ferruzzi, D., Pinna, E., Xompero, Marchetti, E., Fedrigo, E., Le Louarn, M., Madec, P.-Y., Soenke, C., Conzelmann, R., Delabre, B., Hubin, N., "The NGS pyramid wavefront sensor for ERIS," Proc. SPIE 9148, 9148-120 (2014).